JOURNAL OF MATERIALS PROCESSING TECHNOLOGY 199 (2008) 314–320

journal homepage: www.elsevier.com/locate/jmatprotec

# Freeze-dried nanometric neodymium-doped YAG powders for transparent ceramics

Y. Rabinovitch[a,c,*], C. Bogicevic[b], F. Karolak[b], D. Tétard[a], H. Dammak[b]

[a] Université de Limoges, CNRS, UMR no. 6638, Laboratoire Sciences des Procédés Céramiques et de Traitements de Surface, 123 Avenue Albert Thomas, 87060 Limoges Cedex, France
[b] Ecole Centrale de Paris, CNRS, UMR no. 8580, Laboratoire Structure, Propriétés et Modélisation des Solides, Grande Voie des Vignes, 92295 Chatenay-Malabry Cedex, France
[c] CILAS, ESTER Technopole, BP 76923 87069 Limoges Cedex, France

ARTICLE INFO

*Article history:*
Received 2 January 2007
Received in revised form
13 July 2007
Accepted 8 August 2007

*Keywords:*
Transparent ceramic
Sintering
Freeze-drying
Hot isostatic pressing
YAG

ABSTRACT

Nanometric neodymium-doped yttrium aluminium garnet (YAG) has been synthesised from freeze-dried precursors. The products were calcined between 900 °C and 1200 °C under flowing oxygen. Powder morphologies were observed by TEM, SEM and laser granulometer. The oxides had small crystallite size. The best sinterability under vacuum at 1700 °C for 3 h was obtained for precursors with the lowest amount of organic impurities as indicated by IR measurements. Hot isostatic pressing at 1700 °C in 160 MPa of argon was applied to complete the sintering. Under these conditions, Nd:YAG ceramics with very good transmittance were obtained.

© 2007 Elsevier B.V. All rights reserved.

## 1. Introduction

The first undoped translucent yttrium aluminium garnet (YAG) ($Y_3Al_5O_{12}$) ceramic was produced in 1984 by De With and Van Dijk, 1984 who used a solid-state reaction method and a modified sulphate process. In 1995, Ikesue et al. showed that it was possible to obtain a laser effect with a polycrystalline YAG doped with neodymium and synthesised by a solid-state reaction (Ikesue et al., 1995).

To improve laser efficiency, it is well known that a good dispersion of rare earth doping in the matrix avoids concentration quenching. Consequently, synthesis of precursors from the liquid-chemical routes is an alternative to the solid-state reaction process. Indeed, a good distribution of elements at nanometric scale is obtained by these methods. It has been demonstrated that YAG precursors can be obtained by a sol–gel technique such as the citrate gel process (Courty et al., 1973; Vaqueiro and Lopez-Quintela, 1998; Cinibulk, 2000; Roy et al., 1999), or by using yttrium and aluminium alkoxides (Manalert and Rahaman, 1996; Gowda, 1986; Ruan et al., 1998). Another elaboration method is to use the urea (Matsubara et al., 2000; Haneda et al., 1991) or the carbonate precipitation procedure (Li et al., 2000; Lu et al., 2002) to produce nanoparticles. All of these studies demonstrated that it was possible to prepare YAG nanoparticles. But, the sintering of these products was not completed because of the existence of porosity and secondary phases. One team produced transparent YAG from precipitates (Li et al., 2000),

* *Corresponding author at*: CILAS, ESTER Technopole, BP 76923, 87069 Limoges Cedex, France. Tel.: +33 5 55 56 52 61; fax: +33 5 55 56 20 92.
E-mail address: yr@levillage.org (Y. Rabinovitch).
0924-0136/$ – see front matter © 2007 Elsevier B.V. All rights reserved.
doi:10.1016/j.jmatprotec.2007.08.022

but they did not explain how the treatment of their precursors influenced the final optical quality of their ceramics. With the method described in this last work pure YAG phase is obtained for calcination temperature between 950 °C and 1000 °C. The crystallite sizes range from 50 nm to 200 nm when oxidation is realized between 1000 °C and 1300 °C.

To study the role of the precursor-making process on sintering, we have chosen freeze-drying to synthesise the nanoparticles of YAG. This technology has been used by Rasmussen et al. to make $Y_2O_3$ powders. The oxides made in such conditions show one of the best sinterabilities compared to the precursors that were dried differently (Rasmussen et al., 1984). Elsewhere, it has been shown that complex oxides could be synthesised by this method (Bogicevic et al., 2002). Particles obtained from the freeze-drying method are very small and in an amorphous state. With other dehydration processes it is difficult to avoid the particles growth.

Our purpose is to show, first, that freeze-drying can be a useful process for preparing neodymium-doped YAG nanoparticles. Secondly, we will demonstrate that when these precursors are properly treated, they sinter to transparency (Rabinovitch, 2005).

## 2. Experimental procedure

The freeze-drying principle is based on the elimination of water by sublimation of a frozen solution containing cations in stoichiometric ratios. In ceramic powder preparation, this process is useful to produce very thin powders with very good chemical homogeneity (Tretyakov et al., 1997).

The main parameters are

- Chemical compatibility between the salts to avoid undesirable precipitation during their dissolution in the solvent.
- Determination of the solution freezing point which depends on the solvent (water, alcohol, etc.) and the molar concentration of the dissolved species.

This technique is very versatile. It enables us to easily produce very varied compounds if appropriate soluble salts exist.

In our case, aluminium lactate ($(CH_3CH(OH)COO)_3Al$, 95%, Merck), yttrium acetate ($(CH_3CO_2)_3Y$, 99.9%, Chempur) and neodymium acetate ($(CH_3CO_2)_3Nd$, 99.9%, Alfa Aesar) were dissolved in boiling deionised water. High purity acetic acid (99.8% Normapur, Prolabo) was added to maintain the pH of the solution below 4 in order to avoid the precipitation of yttrium lactate ($(CH_3CH(OH)COO)_3Y$). The cation concentrations were calculated to obtain the compound $Nd_{0.03}Y_{2.97}Al_5O_{12}$. Colloidal silica (99.8%, Alfa Aesar) was added as a sintering aid up to 3000 ppm.

First, the boiling solution was sprayed in liquid nitrogen (arrow 1 in Fig. 1). Then, the frozen mass was put on a plate in a freeze-dryer (ALPHA 2–4, Christ) under vacuum (3.5 Pa) (arrow 2 in Fig. 1). By maintaining the temperature of the product at −20 °C for 20 h and the vacuum as low as possible, water was removed by sublimation (arrow 3 in Fig. 1). At the end of the process (arrow 4 in Fig. 1), the product was warmed up to 50 °C to get rid of the adsorbed $H_2O$. We obtained a fluffy powder. If water had remained in it, the solid would melt when returning to ambient temperature and pressure.

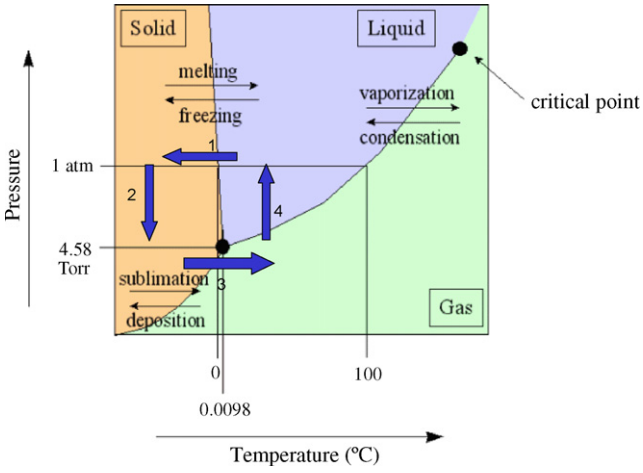


**Fig. 1 – Temperature–pressure diagram of water and representation of a freeze-drying cycle by blue arrows from 1 to 4 (For interpretation of the references to color in this figure legend, the reader is referred to the web version of the article).**

The precursor was inserted in an airtight tubular furnace connected to a high purity oxygen bottle at the input and to a pipe dipping in water at the output. The powder was then oxidized under flowing oxygen between 800 °C and 1200 °C for 1–3 h. As described by Rabinovitch, 2005 calcined powder is ball-milled in deionised water with 1.5 g of oxides for 1 g of 3 mm diameter zirconia beads. After ball-milling, the oxidized powder was uniaxially cold pressed at 300 MPa. The same results were obtained by using cold isostatic pressing. Compacted pellets were sintered under vacuum ($10^{-3}$ Pa) at 1700 °C for 3 h with a heating rate of 5 °C/min. The heating resistance was in tungsten. It was preferred to graphite chamber to avoid the reduction of oxide powders. However, if the sintering process have been realized under air, samples would show less transparency than those treated under vacuum because of remaining pores. The best-sintered samples were treated under hot isostatic pressing (HIP) at 1700 °C under an Ar pressure of 160 MPa for 1.5 h in order to remove the residual porosity. The furnace components of HIP (ACB manufacturer, Alsthom Atlantique) were in graphite, but samples were protected from the reduction by a YAG powder coating.

Oxidized powders were analysed with an infrared (IR) spectrophotometer (IFS 66, Brücker) to detect organic residues. Pellets for IR measurements were prepared as described in the following. These powders were ground with KBr in the amount of 1 wt% of oxide for 99 wt% of KBr. The mixture was then put into a mould and an uniaxial pressure of 400 MPa was applied and maintained for 15 min under vacuum (1 Pa) to remove moisture and carbon dioxide. The pellets were 0.5 mm thick.

Thermogravimetric (TG) analysis (Setaram 92) was performed at 5 °C/min from ambient temperature to 1500 °C. The agglomerate and crystallite sizes were measured by laser granulometer (Mastersizer S, Malvern), scanning electronic microscopy (SEM, LEO 1530) and transmission electronic microscopy (TEM, Philips CM30). The powder was dispersed by ultrasonic device in alcohol, then a droplet of the suspension was put on a copper TEM grid and gently dried.

Powders and sintered body were examined by X-ray diffraction (D5000, Siemens). The absorption spectra was recorded on an UV–vis–NIR spectrophotometer (CARY 5E, Varian).

## 3. Results and discussion

### 3.1. *Freeze-dried and calcined precursors: thermogravimetry (TG) and IR analysis*

TG analysis of this precursor shows that 72% weight loss occurred until complete oxidation (Fig. 2) at 1000 °C. These losses correspond to dehydration and carbonization of the organic molecules as has been shown on similar systems (Todorovsky et al., 2002; Liu et al., 1996).

Organic residues can easily be detected by IR spectroscopy as shown in Fig. 3. The same precursor has been calcined at different temperature from 800 °C to 1100 °C. IR spectra of these powders have been recorded by subtracting the absorption of pure KBr measured in ambient conditions. The plots are normalized on a YAG peak at 568 $cm^{-1}$ to compare the relative absorbance of the organic groups.

Our attention is focused on the characteristic bands, which appear in the range 3200–3400 $cm^{-1}$ related to the H-bonded groups. They can be caused by residual adsorbed water. Hydroxyl groups are detected by IR measurements for samples calcined up to 1000 °C. Only above 1100 °C, it is rather difficult to discern residual water from the ambient moisture. The peaks around 1400 $cm^{-1}$ and 1550 $cm^{-1}$ are related to the $RCO_2^-$ groups. They are related to the organic carboxylic acids remaining in the calcined precursor. Because of the high specific area of the nanopowders, another possibility is that adsorbed atmospheric $CO_2$ has reacted with yttrium to form a

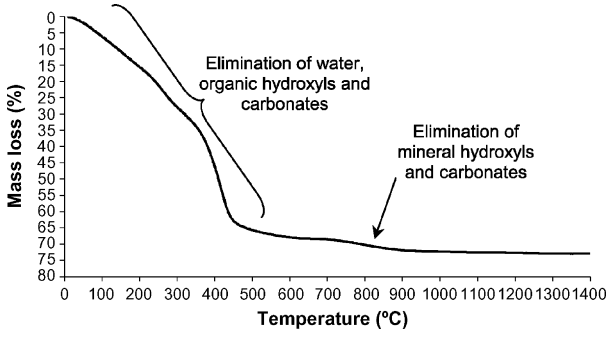


**Fig. 2 – TG analysis of the freeze-dried YAG precursor.**

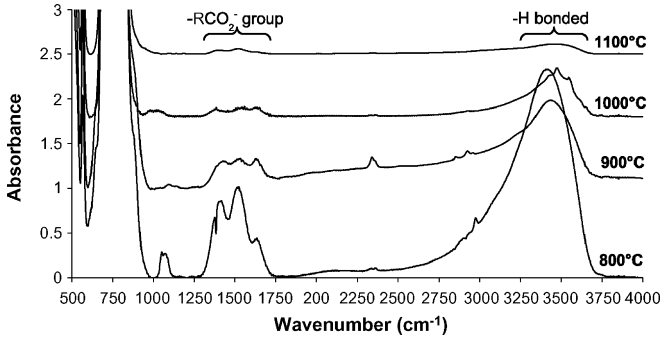


**Fig. 3 – IR spectra of powders as a function of the calcination temperature.**

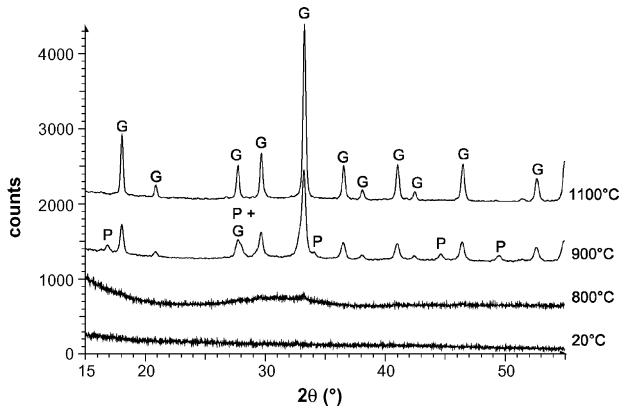


**Fig. 4 – Powder X-ray diffraction diagram as a function of the calcination temperature (G: garnet phase ($Y_3Al_5O_{12}$); P: perovskite phase ($YAlO_3$)).**

stable inorganic complex even after calcination above 1000 °C (Seaverson et al., 1986). In our case, these groups still exist even after a calcination at 1100 °C under air. They are related to rare earth oxycarbonates ($RE_2O_2CO_3$), which are known to be stable up to 800 °C (Brzyska et al., 2001). These results can be compared to the above-mentioned TG analysis in Fig. 2. Indeed, a mass loss of 5% is measured between 700 °C and 800 °C because of the elimination of carbonates. Because weight loss is mainly caused by the formation of gaseous oxides, the oxidation cannot result in a mass growth.

### 3.2. *Grain size and sintering*

Fig. 4 shows the evolution of the X-ray diffraction diagram as a function of the calcination temperature of the precursor. Crystallization begins between 800 °C and 900 °C. At 900 °C, the formation of the YAG phase is almost complete, and a small amount of the YAP phase ($YAlO_3$) is observed. This is much lower than in the case of the solid-state reaction between oxides. In such conditions, YAG is usually formed at 1500–1600 °C (Ikesue et al., 1995).

We can also see that the diffraction peaks become narrower with the elevation of temperature. This is due to the increase of crystallite size $D$ which could be determined by the Scherrer formula using the spherical morphology hypothesis (Guinier, 1956):

$$D = \frac{0.9\lambda}{\cos\theta\sqrt{\Delta_1^2 - \Delta_2^2}}$$

where $\lambda = 1.54$ Å, $\Delta_1$ is the width at half-maximum of a diffraction peak at $\theta$ angle and $\Delta_2$ is the instrumental width of the diffractometer.

Fig. 5 shows the structure of the powders after calcination between 900 °C and 1300 °C under air observed with SEM and TEM. The SEM pictures clearly show agglomerates of the crystallites in the form of plates with an average size of about 1 μm. The crystallite size in these plates grows with heating. Global measurements made with a granulometer (Table 1) reveal that agglomerates become larger when the temperature rises. TEM images show an increase in the crystallite size from 20 to 70 nm after heating at 900 °C to 50–150 nm at 1200 °C. We

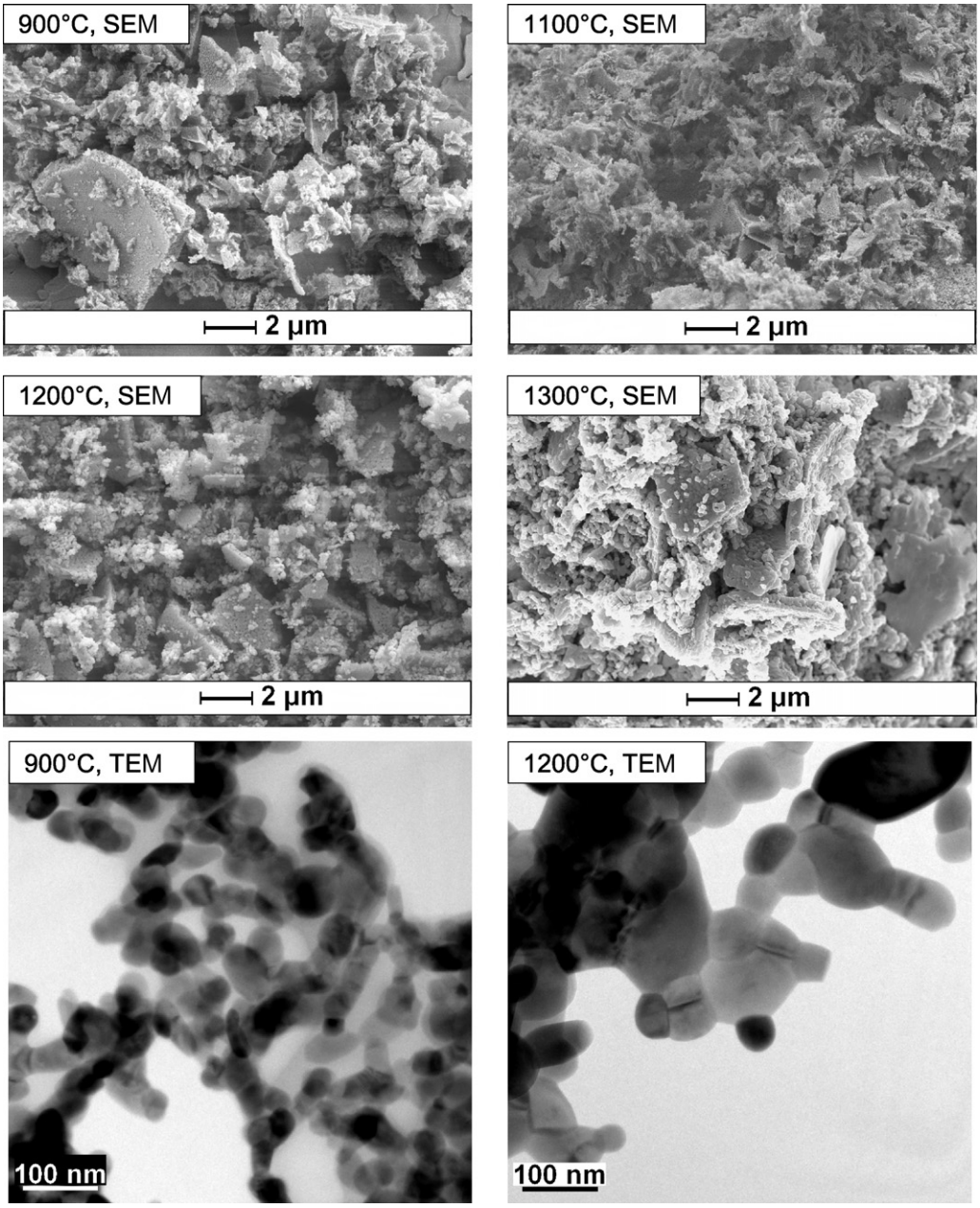


**Fig. 5 – Powder morphology as a function of the calcination temperature observed by HRSEM and TEM.**

**Table 1 – Evolution of crystallite and agglomerates sizes as a function of the temperature (SEM measurements were obtained with image analysis software)**

| Calcination temperature (°C) | Crystallite size (nm) | | Agglomerate size (μm) | | | |
|---|---|---|---|---|---|---|
| | XRD | TEM | SEM | | Laser granulometer | |
| | | | Average diameter | Min–max | d50 | d90 |
| 900 | 30 | 20–70 | 1.18 | 0.2–4.5 | 1.84 | 3.67 |
| 1000 | | | 0.70 | 0.06–3.2 | 2.51 | 4.98 |
| 1100 | 50 | | 1.05 | 0.1–3.4 | 3.11 | 5.62 |
| 1200 | 60 | 50–150 | 0.98 | 0.1–3.3 | 3.26 | 5.86 |
| 1300 | 65 | | 1.61 | 0.1–3.9 | 3.47 | 6.19 |

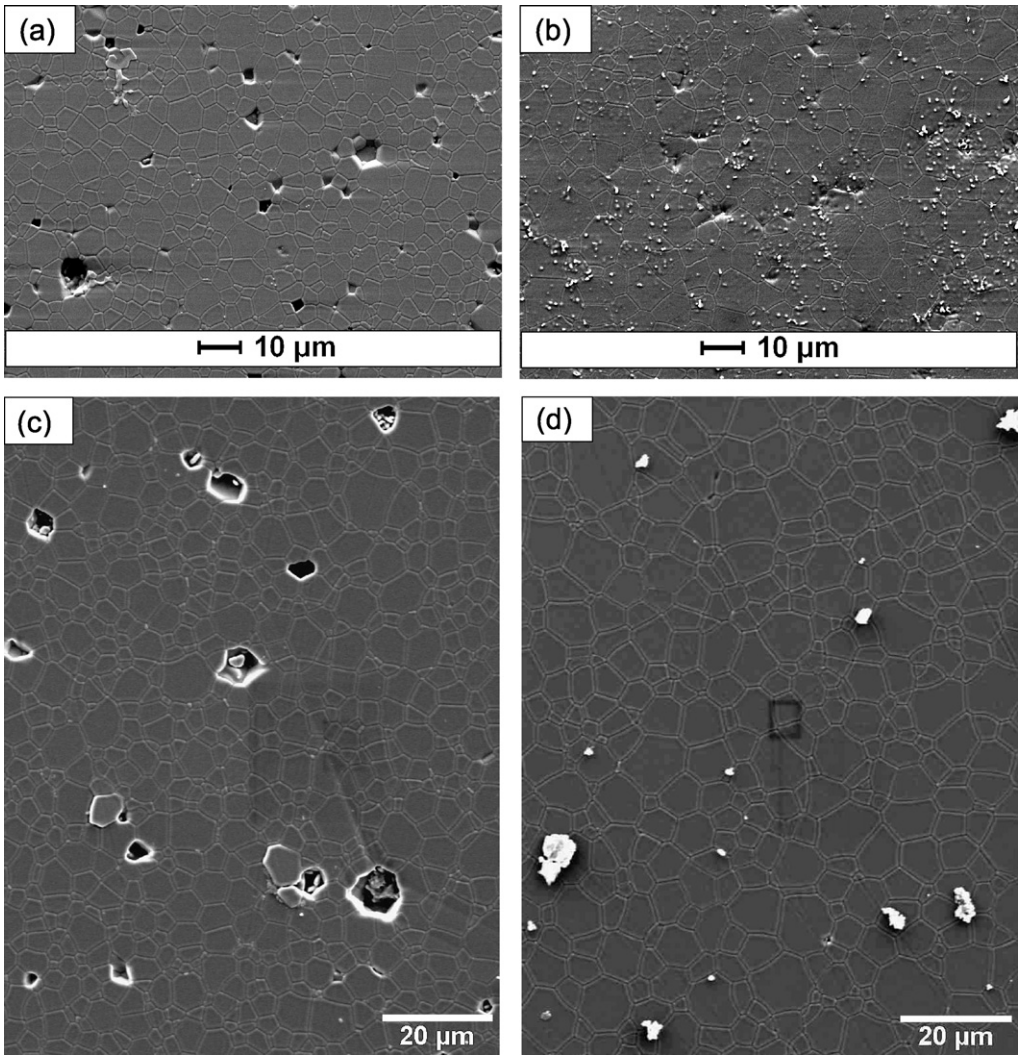


**Fig. 6 – SEM observations of sintered samples (1700 °C, 3 h under vacuum) made from powder oxidized at 1000 °C (a) and 1200 °C (b), and post-HIP samples (1700 °C, 1.5 h in Ar pressure of 160 MPa) made from powder oxidized at 1000 °C (c) and 1200 °C (d).**

notice that these agglomerates are strong enough to resist to the dispersion by ultrasounds.

It is well known that agglomerates prevent sintering as it has been shown earlier on $Y_2O_3$, for example (Sordelet and Akinc, 1988). Consequently, the process to synthesise high sinterability powders must first produce high purity powders, which means a relatively high calcination temperature. But secondly, an agglomerate-free powder with small crystallites has to be obtained to optimise the sinterability. That is to say relatively low-temperature calcination should be performed. So, to obtain optimal properties we have chosen to heat the precursors to between 1000 °C and 1200 °C under flowing oxygen. Such powders exhibit relatively high purity, low agglomeration and small crystallite sizes.

Fig. 6 shows the microstructure of the sintered body after vacuum sintering for 3 h at 1700 °C and the microstructure of the same samples heated in a HIP at 1700 °C for 1.5 h under 160 MPa of Ar. The effect of the calcination temperature of the precursors can be observed. Ceramics made from a powder oxidized at 1000 °C are more porous than those made from a powder oxidized at 1200 °C. This is due to the presence of residual carbonated compounds. When they volatilise during densification, residual pores appear and prevent the complete sintering of the samples. To remove the residual porosity in

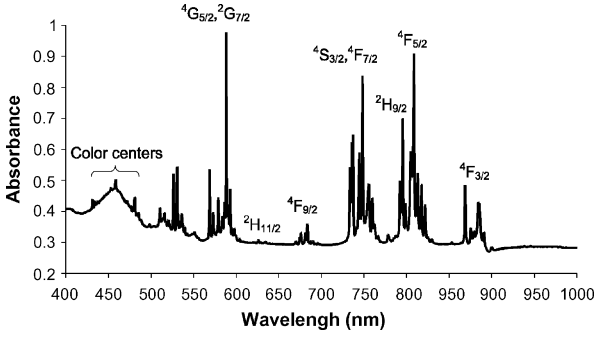


**Fig. 7 – UV–vis absorption spectra of sample shown in Fig. 8 at room temperature (neodymium transitions are labelled from the $^4I_{9/2}$ level).**

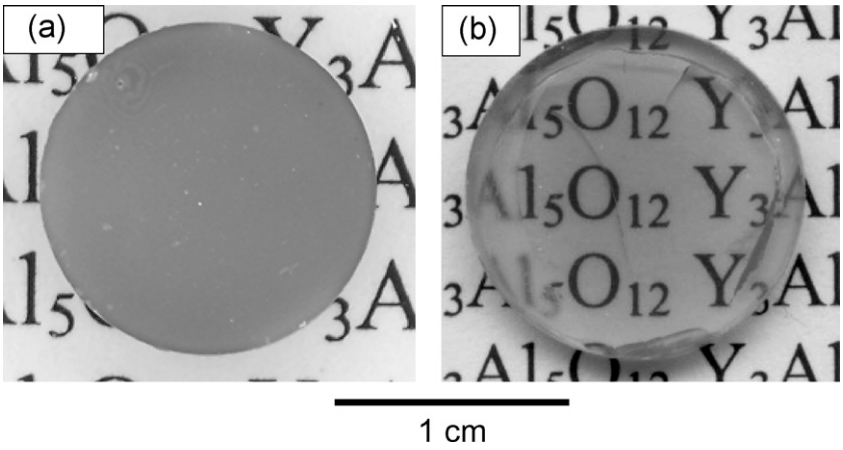


**Fig. 8 – (a) YAG:Nd 2 at.% made from powder calcined at 1000 °C; (b) YAG:Nd 2 at.% sample of 1.6 mm thick, 15 mm diameter made from powder calcined at 1200 °C (both samples vacuum sintered at 1700 °C 3 h + HIP 160 MPa 1700 °C 1.5 h).**

these ceramics, they are post-sintered in a HIP. But, when pores are large and numerous, the HIP is not sufficient to remove all the defects as we can see on the ceramic made from powder calcined at 1000 °C. In the vacuum-sintered ceramic made with a precursor heated at 1200 °C, there are sufficiently few defects for them to be completely eliminated with a HIP procedure. In both cases, the HIP did not affect the average grain size of the ceramic samples.

With powders made from organic precursors, residues, especially carbonates, prevent sintering during vacuum furnace treatment and create porosity. HIP is necessary to realize a pore-free structure.

### 3.3. *Absorption spectra*

The UV–vis absorption spectrum of this sample is shown in Fig. 7. The characteristic lines of neodymium transitions in YAG from the $^4I_{9/2}$ level are detected. But, between 420 nm and 490 nm a large band, which does not belong to the neodymium system appears. Color centers are likely to be responsible for this phenomenon. They can be caused by the incorporation of impurities, such as transition cations, which could be brought in during the process. For optical applications, such as the laser amplifying medium, the elimination of these pollutants will enhance laser efficiency.

Fig. 8 shows a 1.6 mm thick sample of YAG:Nd 2 at.%. It has been sintered under vacuum at 1700 °C for 3 h and hot isostatic pressed at 1700 °C for 1.5 h under 160 MPa of Ar. This sample clearly shows a good transparency.

## 4. Conclusion

Submicronic neodymium-doped YAG ($Y_3Al_5O_{12}$) oxide has been successfully synthesised by calcination of the freeze-dried precursors. The calcination process has been optimised in order to remove, first, all the organic residues and, second, to obtain low agglomerated powders. The powder calcined at 1200 °C, which combines small crystallite size and the lowest amount of organic pollutants, shows the best sinterability. With these oxides, although color centres were detected by transmission, transparent ceramics were obtained after a vacuum sintering at 1700 °C for 3 h completed with a HIP treatment at 1700 °C, 160 MPa of Ar for 90 min.

## REFERENCES

Bogicevic, C., Lahrer-Lacourt, F., Malibert, C., Dkhil, B., Menoret, C., Dammak, H., Giorgi, M.L., Kiat, J.M., 2002. Ferroelectrics 270, 57.
Brzyska, W., Bartyzel, A., Zieniewicz, K., Zwolińska, A., 2001. J. Therm. Anal. Calorim. 63, 493–500.
Cinibulk, M.K., 2000. J. Am. Ceram. Soc. 83 (5), 1276–1278.
Courty, Ph., Ajot, H., Marcilly, Ch., Delmon, B., 1973. Powder Technol. 7 (1), 21–38.
De With, G., Van Dijk, H.J.A., 1984. Mater. Res. Bull. 19, 1669–1674.
Gowda, G., 1986. J. Mater. Sci. Lett. 5 (10), 1029–1032.
Guinier, A., in: Dunod (Ed.), Théorie et technique de la radiocristallographie, 1956.
Haneda, H., Yanagitani, T., Sekita, M., Okamura, F., Shirasaki, S.I., 1991. In: Vincenzini, P. (Ed.), Ceramics Today—Tomorrow's Ceramic, p. 2401.
Ikesue, A., Kinoshita, T., Kamata, K., Yoshida, K., 1995. J. Am. Ceram. Soc. 78 (4), 1033–1040.
Li, J.G., Ikegami, T., Lee, J.H., Mori, T., 2000. J. Am. Ceram. Soc. 83 (4), 961–963.
Liu, Y., Zhang, Z.-F., King, B., Halloran, J., Laine, R.M., 1996. J. Am. Ceram. Soc. 79 (2), 385–394.
Lu, J., Ueda, K.I., Yagi, H., Yanagitani, T., Akiyama, Y., Kaminskii, A.A., 2002. J. Alloys Compd. 341 (1–2), 220–225.
Manalert, R., Rahaman, M.N., 1996. J. Mater. Sci. 31 (13), 3453–3458.
Matsubara, I., Paranthaman, M., Allison, S.W., Cates, M.R., Beshears, D.L., Holcomb, D.E., 2000. Mater. Res. Bull. 35, 217–224.
Rabinovitch, Y., Bogicevic, C., Karolak, F., Dammak, H., French Patent 04 03668 (2005).
Rasmussen, M.D., Akinc, M., Berard, M.F., 1984. Ceram. Int. 10 (3), 99–104.
Roy, S., Wang, L., Sigmund, W., Aldinger, F., 1999. Mater. Lett. 39 (3), 138–141.
Ruan, S.-K., Zhou, J.-G., Zhong, A.-M., Duan, J.-F., Yang, X.-B., Su, M.-Z., 1998. J. Alloys Compd. 275–277, 72–75.

Seaverson, L.M., Luo, S.-Q., Chien, P.-L., McClelland, J.F., 1986. J. Am. Ceram. Soc. 69 (5), 423–429.
Sordelet, D.J., Akinc, M., 1988. J. Am. Ceram. Soc. 71 (12), 1148–1153.
Todorovsky, D.S., Todorovska, R.V., Groudeva-Zotova, St., 2002. Mater. Lett. 55, 41–45.
Tretyakov, Y.D., Oleynikov, N.N., Shlyakhtin, O.A., 1997. Cryochemical Processing of Advanced Materials. Chapman & Hall, London, UK.
Vaqueiro, P., Lopez-Quintela, M.A., 1998. J. Mater. Chem. 8 (1), 161–163.